Journal of Dentistry 148 (2024) 105135

Contents lists available at ScienceDirect

Journal of Dentistry

journal homepage: www.elsevier.com/locate/jdent

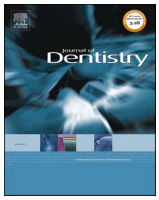

Effect of 3D printer, implant analog and angulation on the accuracy of analog position in implant casts

Vygandas Rutkūnas [a,*], Darius Jegelevičius [b], Agnė Gedrimienė [a], Marta Revilla-León [c,g,h], Justinas Pletkus [a], Mykolas Akulauskas [d], Tan Fırat Eyüboğlu [e], Mutlu Özcan [f], Liudas Auškalnis [a]

[a] Department of Prosthodontics, Institute of Odontology, Faculty of Medicine, Vilnius University, Vilnius, Lithuania
[b] Department of Electronics Engineering, Kaunas University of Technology, Biomedical Engineering Institute, Kaunas, Lithuania
[c] Department of Restorative Dentistry, School of Dental Medicine, University of Washington, Seattle, WA, USA
[d] Kaunas University of Technology, Biomedical Engineering Institute, Lithuania
[e] Department of Endodontics, Faculty of Dentistry, Istanbul Medipol University, Istanbul, Turkey
[f] Clinic of Masticatory Disorders and Dental Biomaterials, Center for Dental Medicine, University of Zurich, Zurich, Switzerland
[g] Kois Center, Seattle, WA, USA
[h] Department of Prosthodontics, Tufts University, Boston, MA, USA

ARTICLE INFO

Keywords:
3D printing
Accuracy
Dental materials
Digital dentistry
Implant analog
Intraoral scanner
Precision
Trueness
Prosthodontics

ABSTRACT

Objectives: To evaluate the accumulative effect of 3D printer, implant analog systems, and implant angulation on the accuracy of analog position in implant casts.

Methods: A reference cast, presenting a case of a three-unit implant-supported prosthesis, was scanned with a coordinate measurement machine, producing the first reference data set (CMM, $n = 1$). The second reference data set ($n = 10$) was prepared using an intraoral scanner (IOS) (Trios4). Test quadrant casts were produced using three DLP type 3D printers, Max (MAX UV385), Pro (PRO 4K65 UV), and Nex (NextDent 5100), and three implant analog systems, El (Elos), Nt (Nt-trading), and St (Straumann) ($n = 90$). Stone casts were also produced via analog impressions (Stone, $n = 10$). After digitization, the accuracy of 3D distance, local angulation (angle between implants) and global angulation (angle between the implant center axis and an axis perpendicular to the global plane) was evaluated by comparing the reference (CMM, IOS), test (3D print), and control (Stone) groups using metrology software. Data were statistically analyzed using three-way ANOVA and Tukey`s tests ($\alpha = 0.05$).

Results: IOS was truer in 3D implant distance and more precise in capturing local angulation than Stone ($p \leq 0.05$). Other measurements were similar between both groups ($p > 0.05$). The amount of error introduced in the workflow by IOS and 3D printing was mostly similar ($p > 0.05$). 3D printed casts had similar or even higher accuracy than Stone group ($p > 0.05$). In most cases, higher trueness was achieved when using PRO 4K65 UV 3D printer and Elos implant analog system ($p \leq 0.05$).

Conclusion: 3D printer, implant analog system, and implant angulation have a significant effect on the accuracy of analog position in implant casts. Limited-span implant-supported cases could be reproduced digitally with similar accuracy as conventional methods.

Clinical significance: A fully digital workflow with a carefully selected 3D printer and implant analog system can increase the accuracy of digitally produced implant casts with comparable accuracy to conventional workflow.

1. Introduction

Inaccuracies in impression-taking and restoration manufacturing can result in implant-prosthesis discrepancies, leading to the formation of micro-gaps and strain [1]. These issues may cause severe biological complications such as peri-implantitis, mucositis, and bone loss, as well

* Corresponding author at. Department of Prosthodontics, Institute of Odontology, Faculty of Medicine, Vilnius University, Zalgirio str. 115, LT-08217 Vilnius, Lithuania.
E-mail address: vygandasr@gmail.com (V. Rutkūnas).

https://doi.org/10.1016/j.jdent.2024.105135
Received 11 February 2024; Received in revised form 4 June 2024; Accepted 14 June 2024
Available online 16 June 2024

as mechanical failures including screw loosening and fractures of prosthetic components [2,3]. Addressing these inaccuracies intraorally, particularly in multiple restorations, is not only time-consuming but also negatively impacts clinical efficiency and patient satisfaction [4,5].

Despite the advancements in digital dentistry that aim to eliminate the need for physical dental casts, these casts remain widely used for adjusting occlusal and proximal contacts, manual veneering, and cementation of the abutments of implant-supported fixed dental prostheses (FDPs) [6]. Stone casts derived from conventional open-tray implant impressions continue to be the standard of care due to their accuracy [7]. However, these casts have several limitations, including time-consuming production processes, potential distortions, and susceptibility to breakage [8,9]. In contrast, digital technologies offer a compelling alternative, providing immediate visualization, enhanced patient comfort, and simplified data storage and sharing [10,11]. In a hybrid digital workflow for producing implant-supported FDPs, physical casts can be 3D printed using intraoral scanner (IOS) data [12,13]. Compared to subtractive methods or traditional techniques, 3D printing offers numerous advantages: it is not restricted by the geometry limitations of milling burs, produces less waste material, and eliminates the generation of grinding dust [14,15]. Among the various 3D printing technologies, Digital Light Processing (DLP) 3D printers are widely used in dental laboratories, operating on the principle of solidifying objects layer by layer in a liquid photopolymer vat using a digital projector [12].

There is no consensus on the clinically acceptable level of implant-prosthesis discrepancy, but linear 100 μm and angular 0.4° are suggested thresholds [16–18]. When casts for implant-supported FDPs are produced via a hybrid workflow, several factors [19–21] - including digital scanning [17], the specific model of a 3D printer [22–24], the implant analog system [25,26], and implant angulation [22,27] - can affect the accuracy of implant analog position in the cast [17,22,25,27]. While the influence of these factors separately has been well researched [28–31], there is a lack of studies evaluating their cumulative effect. Therefore, this study aimed to compare the accuracy (trueness and precision) of implant analog positions in implant casts produced through digital and analog workflows. Additionally, it sought to assess the impact of a 3D printer, implant angulation, and implant analog system on the accuracy of three-unit implant casts derived from IOS data. The first null hypothesis posited that the accuracy of implant analog positions in implant casts fabricated via digital and analog methods would be comparable. The second null hypothesis proposed that the effects of the 3D printer, implant angulation, and implant analog system on the trueness and precision of the implant analog position in dental casts would be negligible.

2. Materials and methods

2.1. Study design

Three types of measurements were conducted: local 3D distance between implants, local angulation between implants, and global angulation. The study scheme is provided in Fig. 1.

2.2. Reference cast

A partially edentulous maxillary cast was additively manufactured (MAX UV385; Asiga, Sydney, Australia) and used as the reference cast. Two dental implants (Bone Level Tapered RC; Straumann, Basel, Switzerland) were inserted in regions 15 and 17. The mesial implant was made perpendicular to the occlusal plane, while the distal implant was angled 5° mesially. Precision spheres (Micro Surface Engineering, Inc., Los Angeles, California), with a diameter of 5 mm, were attached with an auto-polymerizing acrylic resin (Pattern Resin; GC America Inc., Alsip, IL, USA) at the base of the cast (Fig. 2**A**).

2.3. Reference data sets

Titanium scan bodies (3Shape scan body; 3Shape A/S, Copenhagen, Denmark) were torqued with 10 Ncm to the implants. The precision spheres of the reference casts were uniformly coated with a white occlusion spray (O-Spray; S&S Scheftner GmbH, Mainz, Germany). Then, scanning was performed with a coordinate measurement machine (CMM) equipped with an LC15Dx laser scanning head (ALTERA 10.7.6; Nikon Shinagawa, Tokyo, Japan) (Fig. 2B). Data were exported in standard tessellation language (STL) file format, producing the first reference data set (CMM, $n = 1$).

Within 48 h of the CMM scanning, ten digital scans were taken of the reference cast with an IOS (Trios 4, software v.20.1.3; 3Shape A/S) by one experienced clinician, producing a second reference data set (IOS, $n = 10$). Scanning followed the manufacturer's instructions, there was no direct lighting from the chair lamp, no rescanning was needed, the palate was included in the scan, and the device was calibrated every 5 scans.

2.4. Test data set

IOS data was then imported into the CAD (Computer-Aided Design) software (Dental Designer 2021 and Model Builder 2021; 3Shape A/S). Quadrant virtual casts were generated from each scan for each implant analog system (n = 30). Three retrievable implant analog systems were used: Accurate Analog for Printed Models (Elos Medtech, Göteborg, Sweden) (El), DIM-ANALOG (nt-trading GmbH & Co. KG, Karlsruhe, Germany) (Nt), and RC Repositionable Implant Analog (Straumann) (St) (Fig. 2C). After initial testing, the implant analog slot radial offsets were chosen: −30 μm for Nt-trading and −20 μm for Straumann and Elos systems. Hollow digital casts with a 2.5-mm minimum wall thickness were created.

Test casts (Fig. 2D) were then produced with three different DLP-based 3D printers: MAX UV385 (Asiga, firmware 2020-11-13) (Max), PRO 4K65 UV (Asiga, firmware 2020-11-13) (Pro), and NextDent 5100

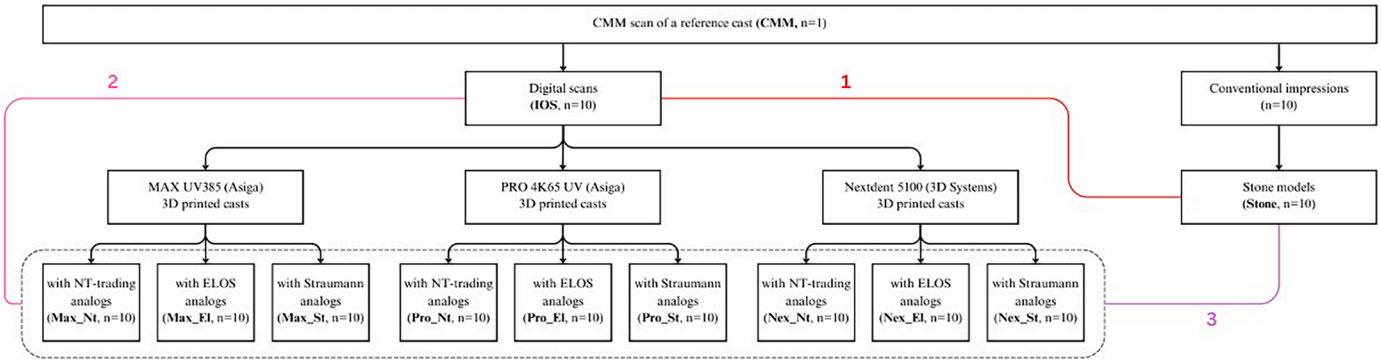

Fig. 1. Flowchart of the experimental procedures. Color lines (marked 1, 2, and 3) represent comparisons between the groups.

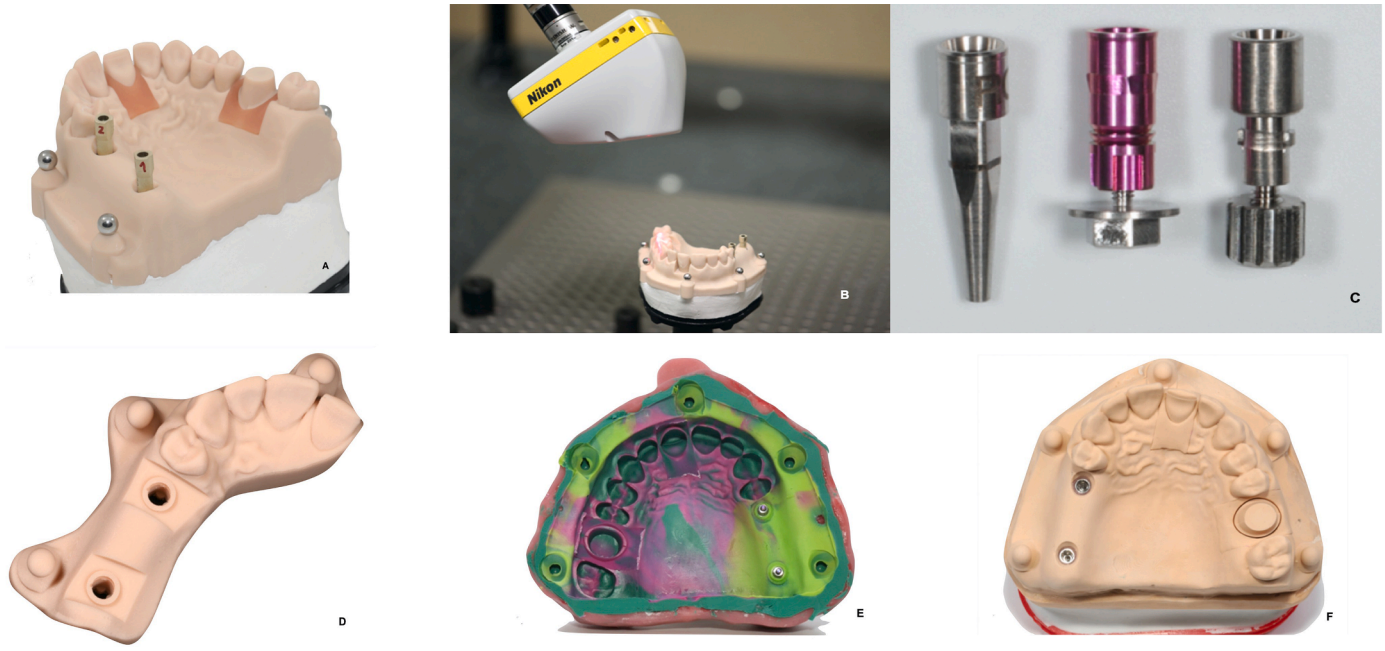

Fig. 2. A, Reference cast. B, Scanning with Nikon Altera CMM. C, Digital implant analogs. D, 3D printed cast. E, Open-tray VPS impression. F, Stone cast.

(3D Systems, firmware v1.1.2, South Carolina, USA) (Nex). DentaMODEL (Asiga) and Model 2.0 (3D Systems) resins were used, according to the manufacturer of the machine. Each cast was positioned horizontally at the center of the build platform and manufactured in a separate print job with a 50 μm layer thickness. 3D printers were calibrated every fifth print, and the post-processing of the casts was carried out strictly following the manufacturers' instructions. Support structures were removed before post-processing. After resting for 1 day at room temperature in a light-proof compartment, 3D printed casts were fitted with digital implant analogs. 3D printing and post-processing of the resin casts, as well as implant analog placement, strictly followed the manufacturers' instructions.

The same scan bodies (3-Shape A/S) were transferred from the reference cast to the 3D printed casts and torqued with 10 Ncm using an electronic screwdriver (iSD900; NSK). 3D printed casts were then digitized with the calibrated laboratory scanner (E4; 3Shape A/S). As a result, 9 digital test data sets (each $n = 10$) of 3D printed casts were generated: Max_Nt, Max_El, Max_St, Pro_Nt, Pro_El, Pro_St, Nex_Nt, Nex_El, and Nex_St (Fig. 1).

2.5. Control data set

Immediately after IOS, conventional impressions (Imprint 4; 3 M ESPE, Saint Paul, Minnesota, United States) of the reference cast ($n = 10$) were taken at room temperature using a double-mix custom tray impression technique (Fig. 2**E**). Open-tray impression abutments (RC Impression Post; Straumann) were torqued with 10 Ncm to the implants using an electronic cordless screwdriver (iSD900; NSK). The impression abutments were splinted with light-polymerizing custom tray material (Individo Lux; VOCO). Impression setting time was set twice as long to compensate for temperature differences between oral and *in vitro* environments.

The impressions were poured with Type IV dental stone (GC Fujirock EP; GC) after mixing under the vacuum (Fig. 2**F**). Stone casts served as a control group. Both impression-making and pouring strictly followed the manufacturers' guidelines. After the casts were fully set, they were digitized with the calibrated laboratory scanner in the aforementioned manner (Stone, $n = 10$) (Fig. 1).

2.6. Measurements

All digital casts were imported into metrology software (Geomagic Control X; 3D Systems). A CAD file of the selected implant scan body (3Shape scan body; 3Shape A/S) was superimposed onto the digital cast. Spherical surfaces were manually selected, and the software automatically detected their center points. Subsequent measurements were conducted in vector space, using only the CAD files of the scan bodies and spheres' center points, excluding the digital cast. This approach enabled automatic selection of points and lines for repeatable measurements. A global plane was drawn through the center points of the three calibration spheres. The local 3D distance was measured between the bottom center points of the implant scan bodies. Local angulation was determined by measuring the angle between the vertical center axes of the scan bodies. A global angulation was also evaluated for each scan body by measuring the angle between the scan body's vertical center axis and a line perpendicular to the global plane. These measurements are illustrated in Fig. 3.

The trueness of the selected test group was evaluated using two reference data sets: CMM and IOS (Fig. 1). Additionally, comparisons within a group were made to evaluate the effect of different 3D printers, digital implant analog systems, and implant angulations, using IOS data as a reference. For precision evaluation, each measured value was subtracted from its respective group means. The absolute values of these differences were used to evaluate the 3D distance, local angulation, and global angulation of mesial and distal implant scan body precision evaluation. The results for each group were summarized using the mean and standard deviation (SD).

2.7. Data analysis

Statistical analysis was performed with a statistical analysis software program (SPSS 27.0; IBM SPSS software; IBM Corporation). All groups were subjected to the Shapiro-Wilk normality test. To verify the homogeneity of variance between category groups, Levene's test was used. An independent two-sample *t*-test was used to estimate the difference between the selected groups' trueness values. An independent Welch's *t*-test was used to estimate the difference between the selected groups precision values. A two-way ANOVA was chosen to evaluate if there is

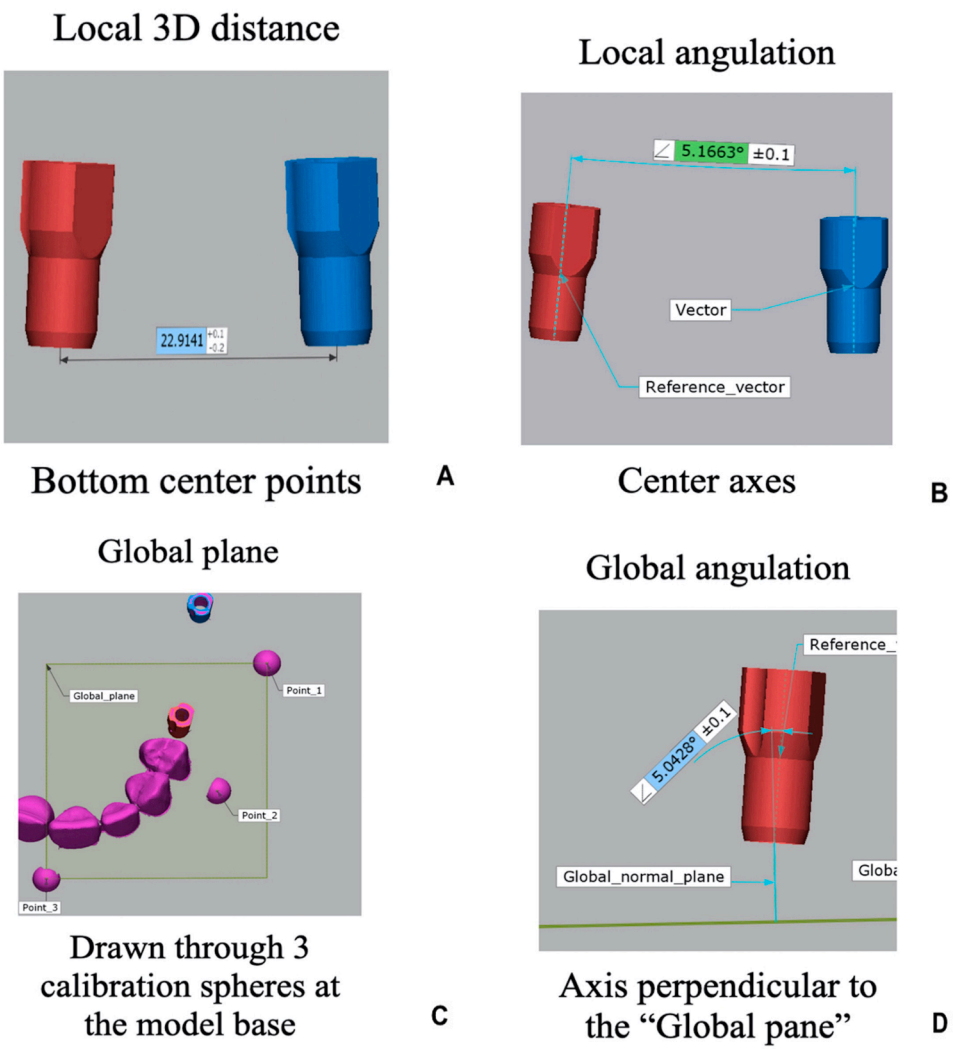

Fig. 3. Illustration of local and global distance and angulation. A, local 3D distance. and B, local angulation. C, Global plane. D, Global angulation.

any interaction between the 3D printer and the implant analog system and their influence on distance, local angulation trueness, and precision values. A three-way ANOVA was used to evaluate global angulation trueness and precision values and the interaction between its factors: the 3D printer, implant analog system, and implant angulation (0° and 5°). A Tukey-HSD post hoc test was used for both factors in the ANOVA. The significance level was set at $\alpha = 0.05$ for all statistical tests.

3. Results

The results (mean and SD) of global and local trueness measurements are presented in Table 1 and precision measurements in Table 2. Figs. 4–7 represent unsigned measurement values. Tables 3, and 4 show Student's t-tests' and Welch's t-tests' *p*-values and differences (Δ) between the groups. Values of comparisons within the groups using two-way, three-way ANOVA, and post-hoc statistical tests are presented for trueness in Tables 5, and 6 and precision in Tables 7 and 8.

3.1. IOS versus stone casts (mutual reference CMM)

The trueness of local 3D distance showed a statistically significant difference between the IOS (20.77 ± 21.33 μm) and Stone groups (Table 3, Fig. 4**a**, 63.88 ± 17.62 μm, $p < 0.001$). Clinically significant trueness deviations were recorded in all angulation measurements of both groups.

When precision was evaluated, only local angulation was significantly different between the IOS and Stone groups (Table 4, Fig. 5**a**, $p = 0.05$, Δ=0.11°). The IOS group (0.13 ± 0.09°) had higher precision than the control group (0.24 ± 0.13°).

3.2. IOS (reference CMM) versus 3D printed casts (reference IOS)

In terms of local 3D distance, 3D printed casts exhibited mostly similar trueness as the IOS group (Table 3, Fig. 4**a**, $p > 0.05$, Δ≤20 μm). In most cases, 3D printing introduced significantly higher local angulation deviations than the IOS step (Table 3, Fig. 5**a**, $p \leq 0.05$, Δ≤−0.31°). Global angulation deviations were mostly statistically insignificantly different between IOS and 3D printed casts (Table 3, $p > 0.05$, Δ≤0.79°).

Further measurements revealed mostly similar precision between IOS and 3D printed casts (Table 4, $p > 0.05$), except for the global angulation precision of the distal scan body. IOS recorded global angulation of the distal scan body with significantly poor precision when compared to reproduction with 3D printing (Table 4, Fig. 7**b**, $p \leq 0.05$, Δ≤0.33°).

3.3. 3D printed casts versus stone casts (mutual reference CMM)

In five out of a total of nine comparisons, 3D printed casts showed significantly better trueness of 3D distance between the implants than

Table 1
Trueness unsigned values (mean ±SD) of local and global measurements.

Reference	Group	Local		Global Angulation	
		3D Distance μm	Angulation °	Mesial SB °	Distal SB °
CMM	IOS	20.77 ± 21.33	0.56 ± 0.17	0.90 ± 0.60	0.55 ± 0.40
	Stone	63.88 ± 17.62	0.58 ± 0.29	0.49 ± 0.31	0.53 ± 0.41
CMM	Max_Nt	52.34 ± 22.34	0.58 ± 0.31	0.81 ± 0.16	0.6 ± 0.37
	Max_El	19.25 ± 18.37	0.81 ± 0.31	0.70 ± 0.21	0.68 ± 0.28
	Max_St	18.76 ± 15.39	0.85 ± 0.22	0.74 ± 0.26	1.10 ± 0.21
	Pro_Nt	71.92 ± 20.11	0.26 ± 0.24	0.11 ± 0.12	0.37 ± 0.25
	Pro_El	19.14 ± 15.39	0.33 ± 0.17	0.86 ± 0.34	0.63 ± 0.29
	Pro_St	22.91 ± 14.65	0.53 ± 0.21	1.24 ± 0.25	1.17 ± 0.25
	Nex_Nt	53.84 ± 27.58	0.46 ± 0.26	0.30 ± 0.23	0.33 ± 0.26
	Nex_El	30.69 ± 21.38	0.81 ± 0.24	0.40 ± 0.14	0.48 ± 0.29
	Nex_St	54.17 ± 22.34	0.87 ± 0.18	0.74 ± 0.39	0.99 ± 0.37
IOS	Max_Nt	67.24 ± 12.89	0.14 ± 0.15	0.42 ± 0.35	0.45 ± 0.38
	Max_El	8.66 ± 11.85	0.34 ± 0.21	0.52 ± 0.40	0.54 ± 0.45
	Max_St	25.05 ± 10.93	0.29 ± 0.18	0.61 ± 0.36	0.78 ± 0.49
	Pro_Nt	92.69 ± 18.11	0.39 ± 0.20	0.99 ± 0.56	0.79 ± 0.48
	Pro_El	14.15 ± 11.50	0.26 ± 0.17	0.58 ± 0.35	0.42 ± 0.37
	Pro_St	36.19 ± 21.52	0.23 ± 0.09	0.63 ± 0.40	0.85 ± 0.54
	Nex_Nt	68.33 ± 29.98	0.34 ± 0.17	0.67 ± 0.59	0.49 ± 0.32
	Nex_El	49.71 ± 20.23	0.25 ± 0.21	0.75 ± 0.55	0.49 ± 0.32
	Nex_St	74.75 ± 16.77	0.31 ± 0.20	0.48 ± 0.36	0.62 ± 0.45

the control group (Table 3, Fig. 4**a**, $p \leq 0.05$, $\Delta \leq 45$ μm). The trueness values of local and global angulation of 3D printed and stone casts were mostly similar (Table 3, $p > 0.05$, $\Delta \leq -0.74°$).

In the current study, the precision of local measurements (3D distance and local angulation) of final 3D printed casts and stone casts was similar (Table 4, Figs. 4**b**, 5**b**, $p > 0.05$, $\Delta \leq -12.06$ μm, $\Delta \leq 0.10°$). However, the opposite was true with global angulation measurements. In most cases, stone casts had significantly poorer precision than 3D printed casts (Table 4, Figs. 6**b**, 7**b**, $p \leq 0.05$, $\Delta \leq 0.32°$).

3.4. Effect of factors: (A) 3D printer; (B) implant analog system; (C) implant angulation

The 3D distance trueness between implant analogs in 3D printed casts was significantly affected by the 3D printer and implant analog system separately ($p < 0.05$) and interactively ($p < 0.001$) (Table 5). Tukey-HSD post hoc tests revealed that Nexdent 5100 (3D Systems) was inferior to MAX UV385 (Asiga) in terms of 3D distance trueness ($p \leq 0.05$) (Table 6). Moreover, there were insignificant differences in 3D distance trueness between the two Asiga 3D printers ($p_{CMM} = 0.49$, $p_{IOS} = 0.18$). As for the implant analog system, DIM-ANALOG (Nt-trading) produced the lowest 3D distance trueness when compared to St and El ($p < 0.001$). However, no significant effect of these factors was detected for the precision of 3D distance (Table 7, $p > 0.05$).

When the CMM data set was considered as a reference, the 3D printer and implant analog system separately showed a significant effect ($p_{CMM} < 0.001$) on the trueness of local angulation. Post-hoc statistical tests showed significantly higher local angulation trueness of the PRO 4K65 UV (Asiga) than the other two tested 3D printers ($p_{CMM} = 0.001$) and of the DIM-ANALOG (Nt-trading) implant analog system than the other two tested analog systems ($p_{IOS} < 0.05$). Furthermore, the precision of local angulation was significantly affected by the implant analog system alone. Analysis showed that the DIM-ANALOG (Nt-trading) implant analog system was significantly less precise than the RC Repositionable Implant Analog (Straumann).

Since the values of global angulation measurements of both implants were merged, a third independent variable was added: implant angulation. Therefore, the three-way ANOVA test was conducted (Tables 5, and 7). Only when CMM was used as a reference did the 3D printer and implant analog system, as separate factors, have a considerable effect on the trueness of global angulation ($p_{CMM} < 0.001$). All combinations of interacting factors (except 3D printer and implant angulation) showed statistical significance ($p_{CMM} < 0.05$). It is evident that Nexdent 5100 (3D Systems) casts presented the highest global angulation trueness (Table 5, $p_{CMM} < 0.05$). As for the implant analog system, DIM-ANALOG (Nt-trading) showed the highest trueness for global angulation, followed by El and St (Table 5, $p_{CMM} < 0.001$). Furthermore, global angulation precision was affected only by the choice of 3D printer (Table 7, $p = 0.05$). Contrary to this, Nexdent 5100 (3D Systems) produced a lower precision of global angulation than MAX UV385 (Asiga).

Table 2
Precision unsigned values (mean ±SD) of local and global measurements.

Group	Local		Global	
	3D Distance μm	Angulation °	Mesial SB °	Distal SB °
IOS	14.33 ± 14.29	0.13 ± 0.09	0.38 ± 0.36	0.47 ± 0.33
Stone	13.95 ± 9.21	0.24 ± 0.13	0.46 ± 0.24	0.44 ± 0.31
Max_Nt	18.88 ± 16.68	0.25 ± 0.14	0.29 ± 0.2	0.14 ± 0.07
Max_El	13.6 ± 17.64	0.27 ± 0.11	0.24 ± 0.13	0.14 ± 0.14
Max_St	18.66 ± 14.72	0.18 ± 0.11	0.17 ± 0.10	0.16 ± 0.19
Pro_Nt	17.05 ± 8.55	0.24 ± 0.17	0.20 ± 0.13	0.12 ± 0.07
Pro_El	13.96 ± 11.91	0.14 ± 0.07	0.23 ± 0.16	0.28 ± 0.15
Pro_St	20.61 ± 12.31	0.15 ± 0.13	0.19 ± 0.14	0.18 ± 0.15
Nex_Nt	26.01 ± 25.4	0.29 ± 0.21	0.25 ± 0.13	0.21 ± 0.15
Nex_El	19.94 ± 10.87	0.21 ± 0.10	0.25 ± 0.17	0.26 ± 0.23
Nex_St	14.56 ± 16.07	0.15 ± 0.09	0.29 ± 0.19	0.30 ± 0.22

4. Discussion

This research aimed to assess the accuracy of implant analog positions within 3D printed casts using three metrics: local distance, local angulation, and global angulation. The initial null hypothesis, proposing that implant analog positions in casts fabricated using digital and analog methods would be comparable, was confirmed. However, the second null hypothesis, which asserted that the impacts of different 3D printers, implant angulations, and implant analog systems would be negligible, was rejected.

The first comparison was made between digital implant scans and stone casts. Digital scans were significantly truer in capturing the 3D distance between the implants and more precise in capturing local angulation than control stone casts. All other measurements showed similar accuracy between IOS and stone casts. Similar observations were made in a study by Bi et al. [32], where different clinical scenarios were tested and compared with conventional casts. The authors conclude that

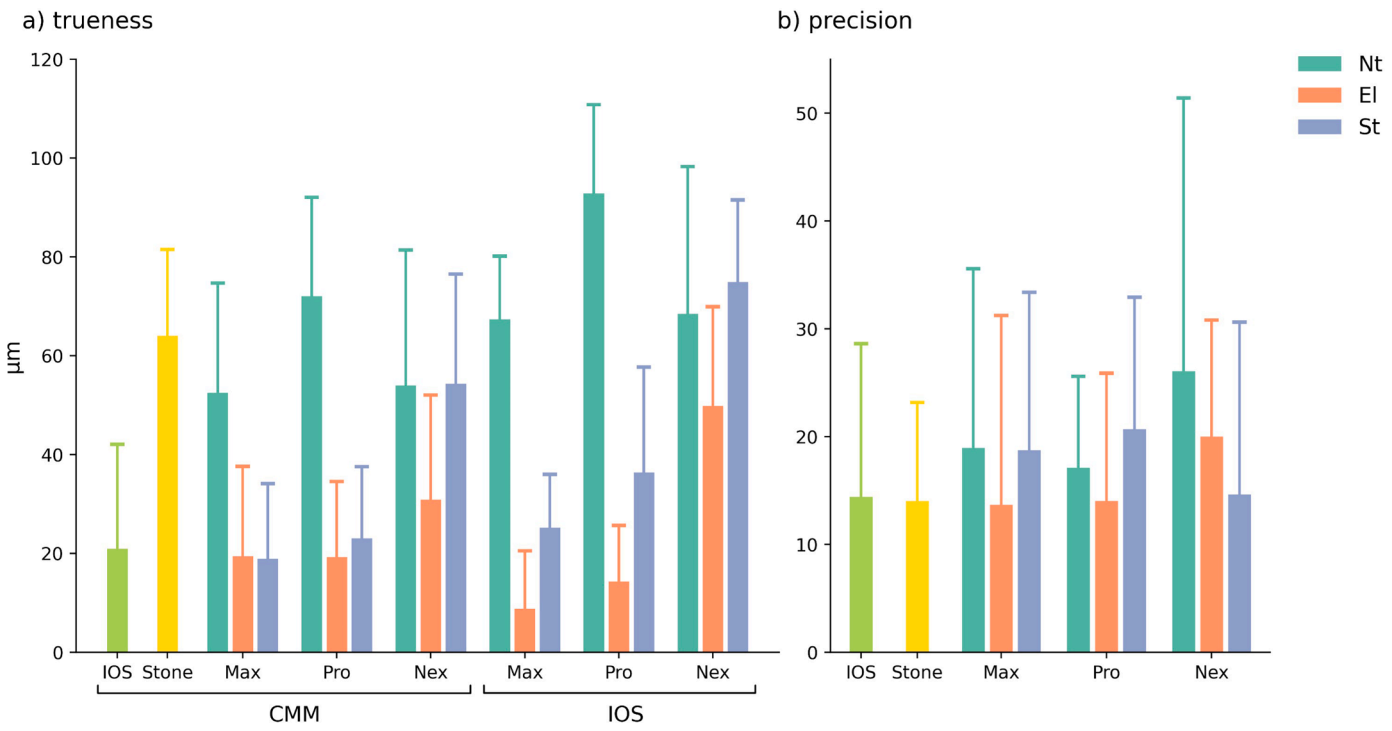

Fig. 4. Unsigned (a) trueness and (b) precision values of 3D distance.

Table 3
Unsigned trueness t-tests' *p*-values and differences (Δ) between Group 1 and Group 2. Positive value showing higher deviations of Group 1. References of the data sets: CMM – black, IOS – green.

Compared groups		Local				Global Angulation			
Group 1	Group 2	3D Distance		Angulation		Mesial SB		Distal SB	
		P	Δ, µm	*P*	Δ,°	*P*	Δ,°	*P*	Δ,°
Stone	IOS	.00*	43*	.84	0.02	.08	−0.40	.89	−0.03
IOS	**Max_Nt**	.00*	−32*	.82	−0.03	.63	0.10	.80	−0.04
	Max_El	.87	20	.03*	−0.26*	.35	0.19	.42	−0.13
	Max_St	.81	20	.00*	−0.29*	.45	0.16	.00*	−0.55*
	Pro_Nt	.00*	−51*	.00*	0.30*	.00*	0.79*	.24	0.18
	Pro_El	.85	20	.01*	0.23*	.87	0.04	.62	−0.08
	Pro_St	.80	−20	.70	0.03	.12	−0.34	.00*	−0.61*
	Nex_Nt	.01*	−33*	.32	0.10	.01*	0.60*	.16	0.22
	Nex_El	.31	−10	.02*	−0.25*	.02*	0.50*	.65	0.07
	Nex_St	.00*	−33*	.00*	−0.31*	.49	0.16	.02*	−0.43*
Stone	Max_Nt	.21	12	.98	0.00	.01*	−0.31*	.69	−0.07
	Max_El	.00*	45*	.09	−0.23	.09	−0.21	.34	−0.16
	Max_St	.00*	45*	.03*	−0.27*	.07	−0.24	.00*	−0.57*
	Pro_Nt	.35	−8	.01*	0.32*	.00*	0.38*	.32	0.15
	Pro_El	.00*	45*	.03*	0.25*	.02*	−0.37*	.51	−0.11
	Pro_St	.00*	41*	.63	0.05	.00*	−0.74*	.00*	−0.64*
	Nex_Nt	.34	10	.34	0.12	.10	0.19	.22	0.20
	Nex_El	.00*	33*	.07	−0.23	.40	0.09	.78	0.05
	Nex_St	.29	10	.02*	−0.29*	.14	−0.24	.02*	−0.46*

*$P \leq .05$.

for unilateral implant cases, a digital scan is equally accurate as an analog workflow.

As a part of the first aim, this study compared digital scans with 3D printed casts, produced with three different DLP-based 3D printers and fitted with implant analogs from three different manufacturers. Since deviations were calculated using two different references (CMM data for the IOS group and IOS for the 3D printer group), it was possible to calculate the introduction of errors at different stages of the digital workflow. The findings showed that the error introduction was mostly similar between the two stages, except for local angulation (where digital scans exhibited higher trueness) and global angulation (where digital scans demonstrated lower precision). Previous research has studied error introduction at different stages of a digital workflow in dentate arches [31]. However, to the authors' knowledge, this is the first study to perform such an analysis on partially edentulous arches with implants.

Furthermore, the primary goal of this study was to compare the final accuracy of implant analog positions in the casts produced using digital and conventional methods. The test group (3D printed casts) showed similar or even higher accuracy compared to the control group (stone casts). All local 3D measurements between the test and control groups showed clinically acceptable trueness and precision (<100 µm) [33]. In

Table 4
Unsigned precision Welch's t-test's *p*-values and differences between Group 1 and Group 2. Positive value showing higher deviations of Group 1.

Compared groups Group 1	Group 2	Local 3D Distance		Angulation		Global Mesial SB		Distal SB	
		P	Δ, μm	*P*	Δ,°	*P*	Δ,°	*P*	Δ,°
Stone	IOS	0.95	−0.37	0.05*	0.11*	0.59	0.08	0.84	−0.03
IOS	Max_Nt	0.54	−4.56	0.05*	−0.12*	0.56	0.08	0.01*	0.33*
	Max_El	0.93	0.72	0.01*	−0.14*	0.31	0.14	0.02*	0.33*
	Max_St	0.53	−4.33	0.37	−0.04	0.13	0.21	0.03*	0.31*
	Pro_Nt	0.63	−2.72	0.10	−0.11	0.20	0.17	0.01*	0.35*
	Pro_El	0.95	0.37	0.86	−0.01	0.30	0.14	0.15	0.18
	Pro_St	0.33	−6.28	0.80	−0.01	0.18	0.18	0.03*	0.29*
	Nex_Nt	0.25	−11.68	0.07	−0.15	0.33	0.13	0.05*	0.26*
	Nex_El	0.36	−5.61	0.11	−0.08	0.36	0.13	0.15	0.20
	Nex_St	0.97	−0.23	0.70	−0.02	0.54	0.09	0.22	0.17
Stone	Max_Nt	0.45	−4.93	0.84	−0.01	0.14	0.16	0.02*	0.30*
	Max_El	0.96	0.35	0.64	−0.03	0.03*	0.22*	0.02*	0.30*
	Max_St	0.43	−4.71	0.26	0.06	0.01*	0.29*	0.04*	0.28*
	Pro_Nt	0.47	−3.10	0.96	0.00	0.02*	0.26*	0.01*	0.32*
	Pro_El	1.00	−0.01	0.06	0.10	0.03*	0.23*	0.21	0.15
	Pro_St	0.21	−6.65	0.14	0.10	0.01*	0.27*	0.04*	0.26*
	Nex_Nt	0.21	−12.06	0.60	−0.04	0.04*	0.21*	0.07	0.23
	Nex_El	0.22	−5.99	0.55	0.03	0.05*	0.21*	0.20	0.17
	Nex_St	0.92	−0.61	0.10	0.09	0.12	0.17	0.29	0.14

*$P \leq .05$.

Table 5
Two-Way and three-Way ANOVA results (∝=0.05) between 3D printed cast groups in terms of trueness. References CMM and IOS.

ANOVA	Two-Way				Three-Way							
Dependent variables:	3D Distance				Local Angulation				Global Angulation			
Reference:	CMM		IOS		CMM		IOS		CMM		IOS	
Source	F	*P*	F	*P*	F	*P*	F	*P*	F	*P*	F	*P*
3D printer	4.82	.01*	21.57	.00*	22.27	.00*	0.55	.58	12.41	.00*	2.03	.14
Implant analogs	26.60	.00*	62.60	.00*	13.17	.00*	0.059	.94	69.39	.00*	1.13	.33
3D printer × Implant analogs	4.23	.00*	10.40	.00*	1.02	.40	3.10	.02*	10.18	.00*	2.38	.05*
Implant angulation	–	–	–	–	–	–	–	–	1.51	.22	0.12	.73
3D printer × Implant angulation	–	–	–	–	–	–	–	–	0.90	.41	0.68	.51
Implant angulation × Implant analogs	–	–	–	–	–	–	–	–	3.01	.05*	2.36	.10
3D printer × Implant angulation × Implant analogs	–	–	–	–	–	–	–	–	3.93	.00*	0.20	.94

*$P \leq .05$.

Table 6
Mean difference and post-hoc Tukey-HSD (∝=0.05) for two-Way and three-Way ANOVA results in terms of trueness. Positive mean difference showing higher deviations of Group 1.

Reference	Measurement		3D printer			Analog system		
		Group 1 Group 2	Max Pro	Max Nex	Pro Nex	El Nt	El St	Nt St
CMM	3D Distance	Mean diff	−7.88	−16.12	−8.24	−36.34	−8.92	27.42
		T-values	−1.15	−2.36	−1.20	−6.29	−1.55	4.75
		P	0.49	0.05*	0.46	0.00*	0.28	0.00*
	Local angulation	Mean diff	0.38	0.03	−0.34	0.22	−0.10	−0.31
		T-values	5.34	0.49	−4.85	2.85	−1.26	−4.10
		P	0.00*	0.86	0.00*	0.02*	0.42	0.00*
	Global angulation	Mean diff	0.04	0.23	0.19	0.21	−0.37	−0.58
		T-values	0.56	3.24	2.68	3.53	−6.21	−9.74
		P	0.83	0.00*	0.02*	0.00*	0.00*	0.00*
IOS	3D Distance	Mean diff	−14.03	−30.61	−16.59	−51.91	−21.16	30.76
		T-values	−1.78	−3.89	−2.11	−8.06	−3.28	4.78
		P	0.18	0.00*	0.09	0.00*	0.00*	0.00*

*$P \leq .05$.

a study by Mathey et al. [34], it was found that implant casts fabricated using a DLP 3D printer had significantly higher trueness compared to stone casts, while the precision between the two groups was similar. Similarly, Banjar et al. [35] found that 3D printed casts with 2 implants placed in the anterior region, produced using both DLP and SLA 3D printers, exhibited higher accuracy than control stone casts. The deviations in test casts produced using the DLP 3D printer were also considered clinically acceptable. However, the type of 3D printer

Table 7
Two-Way and three-Way ANOVA results (∝=0.05) between 3D printed cast groups in terms of precision.

ANOVA	Two-Way				Three-Way	
Dependent variables:	3D Distance		Local Angulation		Global Angulation	
Source	F	P	F	P	F	P
3D printer	0.34	0.71	1.24	0.29	3.11	0.05*
Implant analogs	0.64	0.53	4.12	0.02*	0.64	0.53
3D printer × Implant analogs	0.65	0.63	0.61	0.65	1.28	0.28
Implant angulation	–	–	–	–	2.11	0.15
3D printer × Implant angulation	–	–	–	–	1.17	0.31
Implant angulation × Implant analogs	–	–	–	–	1.36	0.26
3D printer × Implant angulation × Implant analogs	–	–	–	–	0.35	0.84

*$P \leq .05$.

significantly affected accuracy, with lower accuracy observed when using the SLA 3D printing technique [35]. Both aforementioned studies evaluated the accuracy indirectly by measuring the surface deviations of the scan bodies attached to the implants. Additionally, Revilla-León et al. [33] and Bohner et al. [36] found that positional accuracy of implant analogs in casts manufactured using either DLP or SLA methodologies was comparable to conventional methods.

The secondary aim of this study was to investigate the effect of three independent variables: DLP-based 3D printer, implant analog system, and implant angulation. It was evident that the choice made by the operator could significantly influence the accuracy of the implant analog positions in the implant casts. 3D printers influenced almost all measurements, except for local precision. The best trueness of local measurements was achieved by PRO 4K65 UV (Asiga) rather than MAX UV385 (Asiga) or NextDent 5100 (3D Systems). As for the implant analog system, DIM-ANALOG (Nt-trading) achieved the highest angulation trueness but the worst 3D distance trueness. Other measurements showed conflicting results. Similar results were reported by Maria et al. [26], who observed a significant effect of the choice of implant analog system on the accuracy of 3D printed casts. The authors reported that 3D printing build orientation, even though significant, had no discernible trends. Different analog holder radial offsets had insignificant effects on the trueness of the 3D printed casts. According to these results, second null hypothesis was completely rejected for trueness and partially rejected for precision.

This study presents valuable insights, yet certain limitations must be

Table 8
Mean difference and post-hoc Tukey-HSD (∝=0.05) for two-Way and three-Way ANOVA results in terms of precision. Positive mean difference showing higher deviations of Group 1.

Measurement		3D printer			Analog system		
	Group1 Group2	Max Pro	Max Nex	Pro Nex	El Nt	El St	Nt St
Local Angulation	Mean diff	–	–	–	−0.06	0.05	0.10
	T-values	–	–	–	−1.56	1.32	2.88
	P	–	–	–	0.27	0.39	0.01*
Global angulation	Mean diff	−0.01	−0.07	−0.06	–	–	–
	T-values	−0.36	−2.32	−1.95	–	–	–
	P	0.90	0.05*	0.13	–	–	–

*$P \leq .05$.

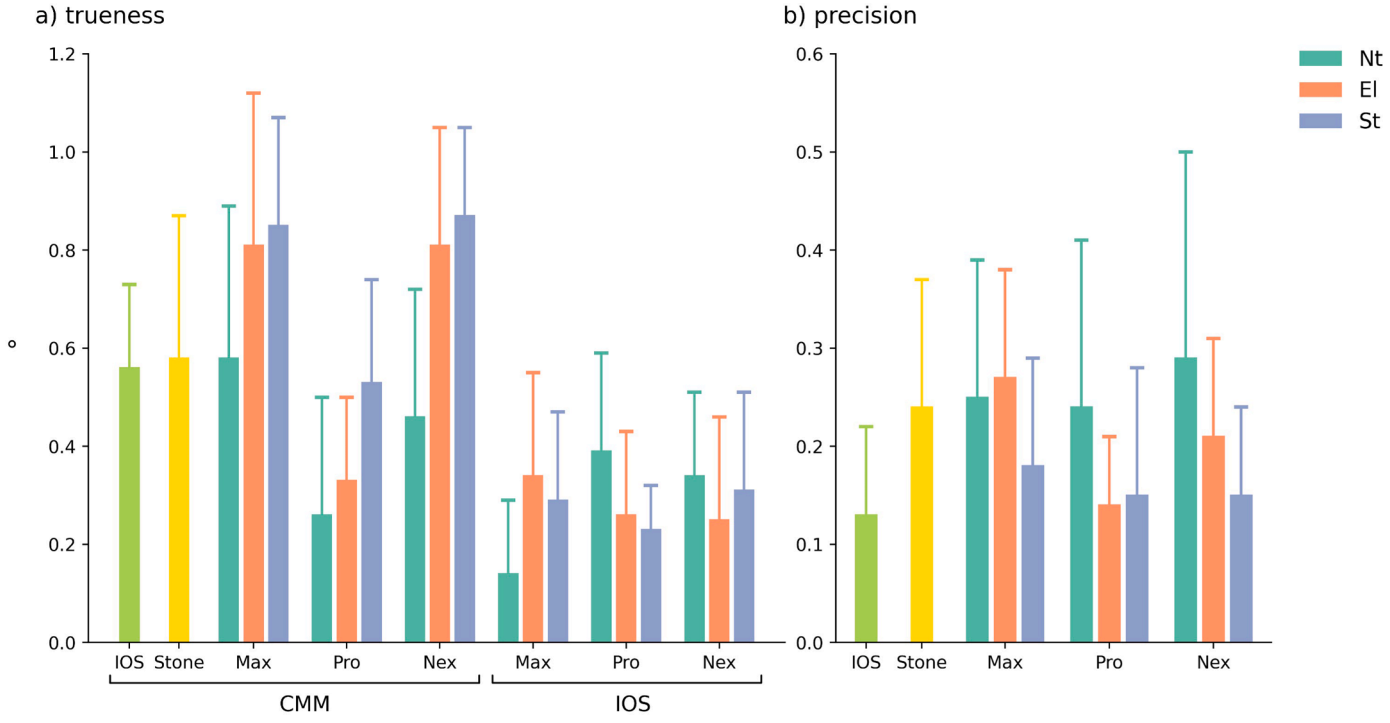

Fig. 5. Unsigned (a) trueness and (b) precision values of Local Angulation.

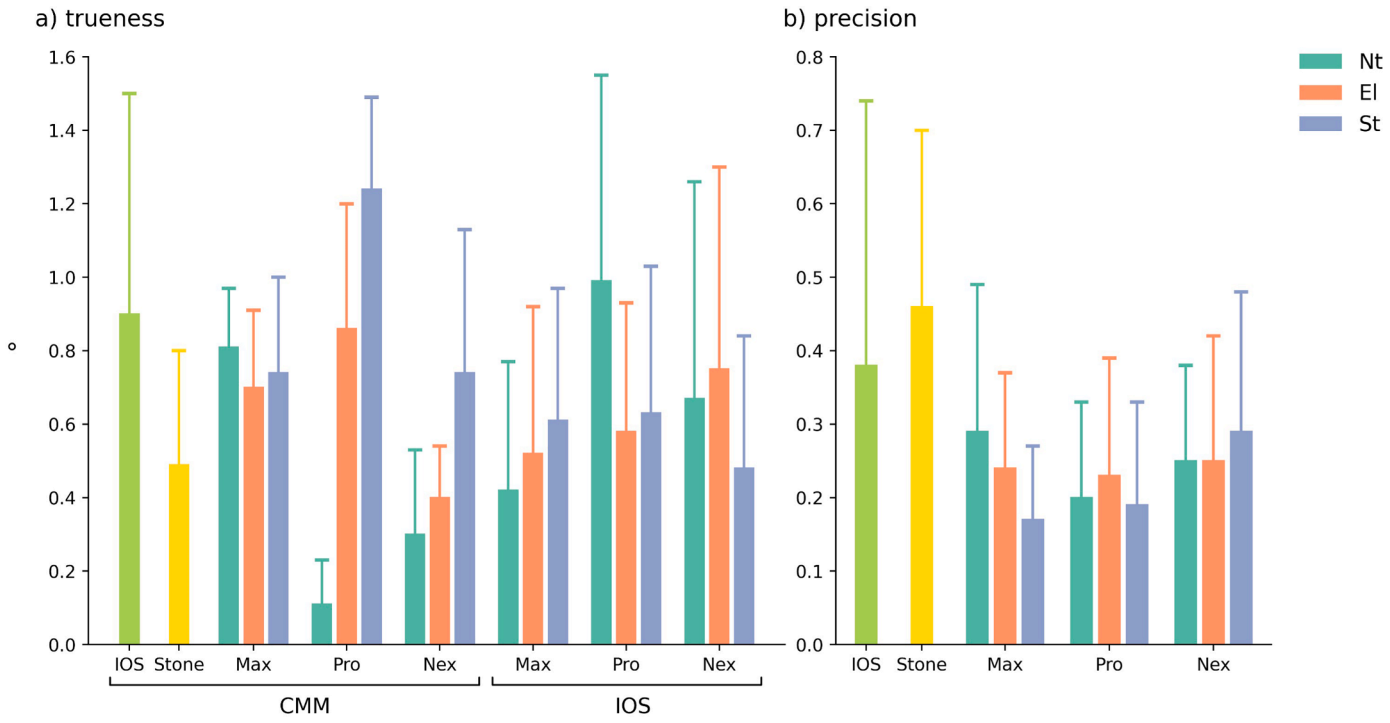

Fig. 6. Unsigned (a) trueness and (b) precision values of Global Angulation of the mesial implant.

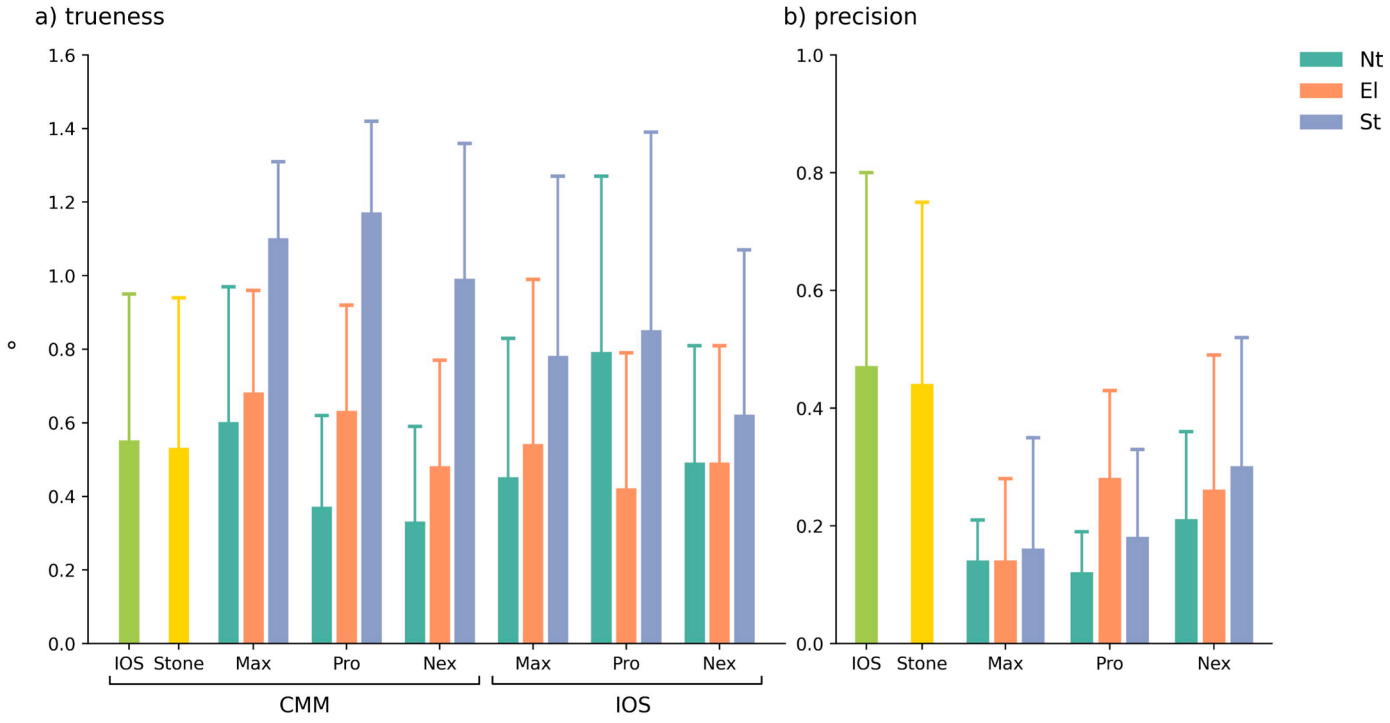

Fig. 7. Unsigned (a) trueness and (b) precision values of Global Angulation of the distal implant.

recognized. These include the in vitro study design, the use of a laboratory scanner, a limited number of digital devices tested, and the indirect measurement of position accuracy through scan bodies. In vivo, IOS accuracy can be influenced by factors such as saliva, movable soft tissues, and the accessibility of scanning areas. The laboratory scanner, despite its manufacturer-specified accuracy of 4 μm [37], can introduce deviations. The combination of different IOSs and 3D printers can also lead to varying accuracy results. Additionally, using the same implant scan bodies may have introduced repositioning inaccuracies. The study did not evaluate other factors identified by previous research, such as 3D printing layer thickness, build orientation, 3D printer technology, model resin, and the software used for accuracy analysis, which can impact the final accuracy of 3D-printed dental casts.

5. Conclusions

Based on the findings of this study, it can be concluded that the accuracy of implant analog positions in implant casts fabricated via digital methods was, in most cases, comparable to or even higher than that of stone casts. Additionally, it was evident that the choice of 3D printer, implant analog system, and implant angulation significantly impacted the trueness of implant analog positions in the casts, while their effect on precision was negligible.

Funding

The study was supported by the Lithuanian Business Support Agency grant Nr. J05-LVPA-K-01-055 and DIGITORUM research team registration number "MTTP SK".

CRediT authorship contribution statement

Vygandas Rutkūnas: Writing – review & editing, Writing – original draft, Validation, Supervision, Resources, Methodology, Investigation, Funding acquisition, Conceptualization. **Darius Jegelevičius:** Writing – original draft, Validation, Supervision, Methodology, Data curation, Conceptualization. **Agnė Gedrimienė:** Writing – original draft, Methodology, Investigation, Data curation. **Marta Revilla-León:** Writing – original draft, Validation, Supervision, Conceptualization. **Justinas Pletkus:** Writing – original draft, Methodology, Investigation, Data curation. **Mykolas Akulauskas:** Writing – original draft, Methodology, Formal analysis, Data curation. **Tan Fırat Eyüboğlu:** Writing – review & editing, Writing – original draft, Validation. **Mutlu Özcan:** Writing – review & editing, Writing – original draft, Validation. **Liudas Auškalnis:** Writing – original draft, Methodology, Investigation, Data curation.

Declaration of competing interest

The authors declare that they have no known competing financial interests or personal relationships that could have appeared to influence the work reported in this paper.

The author is an Editorial Board Member/Editor-in-Chief/Associate Editor/Guest Editor for *Journal of Dentistry* and was not involved in the editorial review or the decision to publish this article.

References

[1] V. Rutkūnas, A. Gečiauskaitė, D. Jegelevičius, M. Vaitiekūnas, Accuracy of digital implant impressions with intraoral scanners. A systematic review, Eur. J. Oral Implantol. 10 (2017) 101–120.
[2] J. Katsoulis, T. Takeichi, A. Sol Gaviria, L. Peter, K. Katsoulis, Misfit of implant prostheses and its impact on clinical outcomes. Definition, assessment and a systematic review of the literature, Eur. J. Oral Implantol. 10 (2017) 121–138.
[3] M. Karl, T.D. Taylor, Bone adaptation induced by non-passively fitting implant superstructures: a randomized clinical trial, Int. J. Oral. Max. Impl. 31 (2016) 369–375.
[4] P. Papaspyridakos, K. Vazouras, Y.W. Chen, E. Kotina, Z. Natto, K. Kang, et al., Digital vs conventional implant impressions: a systematic review and meta-analysis, J. Prosthodont. 29 (2020) 660–678, https://doi.org/10.1111/jopr.13211.
[5] A. Marghalani, H.P. Weber, M. Finkelman, Y. Kudara, K. El Rafie, P. Papaspyridakos, Digital versus conventional implant impressions for partially edentulous arches: an evaluation of accuracy, J. Prosthet. Dent. 119 (2018) 574–579, https://doi.org/10.1016/j.prosdent.2017.07.002.
[6] H. Parize, J. Dias Corpa Tardelli, L. Bohner, N. Sesma, V.A. Muglia, A. Cândido Dos Reis, Digital versus conventional workflow for the fabrication of physical casts for fixed prosthodontics: a systematic review of accuracy, J. Prosthet. Dent. 128 (2021) S0022–391330798–8, https://doi.org/10.1016/j.prosdent.2020.12.008.
[7] P. Papaspyridakos, C.J. Chen, G.O. Gallucci, A. Doukoudakis, H.P. Weber, V. Chronopoulos, Accuracy of implant impressions for partially and completely edentulous patients: a systematic review, Int. J. Oral. Max. Impl. 29 (2014) 836–845.
[8] A. Bhargav, V. Sanjairaj, V. Rosa, L.W. Feng, J.Fuh Yh, Applications of additive manufacturing in dentistry: a review, J. Biomed. Mater. Res. B App. Biomater. 106 (2018) 2058–2064, https://doi.org/10.1002/jbm.b.33961.
[9] M. Javaid, A. Haleem, Current status and applications of additive manufacturing in dentistry: a literature-based review, J. Oral Biol. Craniofac. Res. 9 (2019) 179–185.
[10] F. Mangano, A. Gandolfi A, G. Luongo, S. Logozzo, Intraoral scanners in dentistry: a review of the current literature, BMC Oral Health 17 (2017) 149, https://doi.org/10.1186/s12903-017-0442-x.
[11] H. Kihara, W. Hatakeyama, F. Komine, K. Takafuji, T. Takahashi, J. Yokota, K. Oriso, H. Kondo, Accuracy and practicality of intraoral scanner in dentistry: a literature review, J. Prosthodon. Res. 64 (2020) 109–113, https://doi.org/10.1016/j.jpor.2019.07.010.
[12] D. Khorsandi, A. Fahimipour, P. Abasian, S.S. Saber, M. Seyedi, S. Ghanavati, et al., 3D and 4D printing in dentistry and maxillofacial surgery: printing techniques, materials, and applications, Acta Biomater. 122 (2021) 26–49, https://doi.org/10.1016/j.actbio.2020.12.044.
[13] M. Revilla-León, M. Sadeghpour, M. Özcan, An update on applications of 3D printing technologies used for processing polymers used in implant dentistry, Odontology 108 (2020) 331–338, https://doi.org/10.1007/s10266-019-00441-7.
[14] M. Braian, R. Jimbo, A. A. Wennerberg, Production tolerance of additive manufactured polymeric objects for clinical applications, Dent. Mater. 32 (2016) 853–861, https://doi.org/10.1016/j.dental.2016.03.020.
[15] S. Bukhari, B.J. Goodacre, A. AlHelal, M.T. Kattadiyil, P.M. Richardson, Three-dimensional printing in contemporary fixed prosthodontics: a technique article, J. Prosthet. Dent. 119 (2018) 530–534, https://doi.org/10.1016/j.prosdent.2017.07.008.
[16] J. Abduo, V. Bennani, N. Waddell, K. Lyons, M. Swain, Assessing the fit of implant fixed prostheses: a critical review, Int. J. Oral. Max. Impl. 25 (2010) 506–515.
[17] F.S. Andriessen, D.R. Rijkens, W.J. van der Meer, D.W. Wismeijer, Applicability and accuracy of an intraoral scanner for scanning multiple implants in edentulous mandibles: a pilot study, J. Prosthet. Dent. 111 (2014) 186–194, https://doi.org/10.1016/j.prosdent.2013.07.010.
[18] A. Gedrimiene, R. Adaskevicius, V. Rutkunas, Accuracy of digital and conventional dental implant impressions for fixed partial dentures: a comparative clinical study, J. Adv. Prosthodont. 11 (2019) 271–279, https://doi.org/10.4047/jap.2019.11.5.271.
[19] M. Revilla-León, W. Piedra-Cascón, R. Aragoneses, M. Sadeghpour, B.A. Barmak, A. Zandinejad, et al., Influence of base design on the manufacturing accuracy of vat-polymerized diagnostic casts: an in vitro study, J. Prosthet. Dent. (2021) S0022–391300254-7, https://doi.org/10.1016/j.prosdent.2021.03.035.
[20] S.H. Shin, J.H. Lim, Y.J. Kang, J.H. Kim, J.S. Shim, J.E. Kim, Evaluation of the 3D printing accuracy of a dental model according to its internal structure and cross-arch plate design: an in vitro study, Materials (Basel) 13 (2020) 5433, https://doi.org/10.3390/ma13235433.
[21] N. Alharbi, R.B. Osman, D. Wismeijer, Factors influencing the dimensional accuracy of 3d-printed full-coverage dental restorations using stereolithography technology, Int. J. Prosthodont. 29 (2016) 503–510, https://doi.org/10.11607/ijp.4835.
[22] B. Gimenez-Gonzalez, B. Hassan, M. Özcan, G. Pradíes, An in vitro study of factors influencing the performance of digital intraoral impressions operating on active wavefront sampling technology with multiple implants in the edentulous maxilla, J. Prosthodont. 26 (2017) 650–655, https://doi.org/10.1111/jopr.12457.
[23] R.B. Osman, N. Alharbi, D. Wismeijer, Build angle: does it influence the accuracy of 3d-printed dental restorations using digital light-processing technology? Int. J. Prosthodont. 30 (2017) 182–188, https://doi.org/10.11607/ijp.5117.
[24] D. Mostafavi, M.M. Methani, W. Piedra-Cascón, A. Zandinejad, W. Att, M. Revilla-León, Influence of the polymerization post-processing procedures on the accuracy of additively manufactured dental model material, Int. J. Prosthodont. 36 (2023) 479–485, https://doi.org/10.11607/ijp.7349.
[25] M. Revilla-León, R. Fogarty, J.J. Barrington, A. Zandinejad, M. Özcan, Influence of scan body design and digital implant analogs on implant replica position in additively manufactured casts, J. Prosthet. Dent. 124 (2020) 202–210, https://doi.org/10.1016/j.prosdent.2019.07.011.
[26] R. Maria, M.Y. Tan, K.M. Wong, B.C.H. Lee, V.A.P. Chia, K.B.C. Tan, Accuracy of implant analogs in 3d printed resin models, J. Prosthodont. 30 (2021) 57–64, https://doi.org/10.1111/jopr.13217.
[27] L. Arcuri, A. Pozzi, F. Lio, E. Rompen, W. Zechner, A. Nardi, Influence of implant scanbody material, position and operator on the accuracy of digital impression for complete-arch: a randomized in vitro trial, J. Prosthodont. Res. 64 (2020) 128–136, https://doi.org/10.1016/j.jpor.2019.06.001.
[28] Y. Etemad-Shahidi, O.B... Qallandar, J. Evenden, F. Alifui-Segbaya, K.E. Ahmed, Accuracy of 3-dimensionally printed full-arch dental models: a systematic review, J. Clin. Med. 20 (2020) 3357, https://doi.org/10.3390/jcm9103357.
[29] International Organization for Standardization. ISO 5725-1:1994. Accuracy (trueness and precision) of measurement methods and result – Part 1: general principles and definition. 1994. Available at: https://www.iso.org/obp/ui/#iso:std:iso:5725:-1:ed-1:v1:en.
[30] S.J. Mata-Mata, M.B. Donmez, L. Meirelles, W.M. Johnston, B. Yilmaz, Influence of digital implant analog design on the positional trueness of an analog in additively manufactured models: an in-vitro study, Clin. Implant. Dent. Relat. Res. 24 (2022) 821–830, https://doi.org/10.1111/cid.13137.
[31] L. Auškalnis, M. Akulauskas, D. Jegelevičius, T. Simonaitis, V. Rutkūnas, Error propagation from intraoral scanning to additive manufacturing of complete-arch dentate models: an in vitro study, J. Dent. 121 (2022) 104136, https://doi.org/10.1016/j.jdent.2022.104136.
[32] C. Bi, X. Wang, F. Tian, Z. Qu, J. Zhao, Comparison of accuracy between digital and conventional implant impressions: two and three dimensional evaluations, J. Adv. Prosthodont. 14 (2022) 236–249, https://doi.org/10.4047/jap.2022.14.4.236.

[33] M. Revilla-León, Ó. Gonzalez-Martín, J. Pérez López, J.L. Sánchez-Rubio, M. Özcan, Position accuracy of implant analogs on 3D printed polymer versus conventional dental stone casts measured using a coordinate measuring machine, J. Prosthodont. 27 (2018) 560–567. http://orcid.org/0000-0003-2854-1135.
[34] A. Mathey, U. Brägger, T. Joda, Trueness and precision achieved with conventional and digital implant impressions: a comparative investigation of stone versus 3-d printed master casts, Eur. J. Prosthodont. Restor. Dent. 29 (2021), https://doi.org/10.1922/ejprd_2114mathey08.
[35] A. Banjar, Y.W. Chen, A. Kostagianni, M. Finkelman, A. Papathanasiou, K. Chochlidakis, P. Papaspyridakos, Accuracy of 3D printed implant casts versus stone casts: a comparative study in the anterior maxilla, J. Prosthodont. 30 (2021) 783–788, https://doi.org/10.1111/jopr.13335.
[36] L. Bohner, M. Hanisch, G. De Luca Canto, E. Mukai, N. Sesma, P.T. Neto, Accuracy of casts fabricated by digital and conventional implant impressions, J. Oral Implantol. 45 (2019) 94–99, https://doi.org/10.1563/aaid-joi-D-17-00142.
[37] A New E4 lab scanner is released - 3Shape Press, 3Shape (n.d.). https://www.3shape.com/en/press/2019/double-up-your-labs-scanning-speed-and-accuracy (accessed September 19, 2023).